Quaternary Science Reviews 225 (2019) 106020

Contents lists available at ScienceDirect

Quaternary Science Reviews

journal homepage: www.elsevier.com/locate/quascirev

La Niña-driven flooding in the Indo-Pacific warm pool during the past millennium

Jessica R. Rodysill [a, b, *], James M. Russell [a], Mathias Vuille [c], Sylvia Dee [a, d], Brent Lunghino [a], Satria Bijaksana [e]

[a] Dept. of Earth, Environmental, and Planetary Sciences, Brown University, 324 Brook Street, Providence, RI 02912, USA
[b] U.S. Geological Survey, Florence Bascom Geoscience Center, 12201 Sunrise Valley Dr., MS926A, Reston, VA 20192, USA
[c] Dept. of Atmospheric and Environmental Sciences, University at Albany, 1400 Washington Ave., Albany, NY 12222, USA
[d] Dept. of Earth, Environmental, and Planetary Sciences, Rice University, 6100 Main Street, Houston, TX 77005, USA
[e] Faculty of Mining and Petroleum Engineering, Institut Teknologi Bandung, Jalan Ganesa 10, Bandung 40132, Indonesia

ARTICLE INFO

Article history:
Received 19 July 2019
Received in revised form
15 October 2019
Accepted 17 October 2019
Available online xxx

Keywords:
Floods
Pacific Ocean
Climate
Indonesia
Precipitation
La Niña

ABSTRACT

Extreme precipitation events are one of the most consequential components of climate change for society. The El Niño-Southern Oscillation (ENSO) is the dominant mode of precipitation variability in the tropics and causes severe flooding and drought in many socioeconomically vulnerable regions. It remains unclear how tropical rainfall extremes and ENSO are changing in response to anthropogenic forcing, demanding that we investigate the relationships between precipitation, ENSO, and external forcing in the past. Lake sediment records have provided benchmark records of extreme flood events from the eastern tropical Pacific, where paleofloods have been interpreted to reflect El Niño events during the last millennium. However, the connections between flooding and ENSO variability in this region are uncertain, and the eastern Pacific can only capture precipitation events driven by El Niño, not La Niña. Thus, it is unclear how the ENSO system and tropical rainfall extremes have changed in the recent past. Here, we reconstruct flood events during the past millennium using a lake sediment record from East Java, Indonesia, which can provide insight into flooding driven by La Niña. We detect flood frequency variations in the western tropical Pacific that are highly coherent with records from the eastern part of the basin over the past millennium. Our findings demonstrate that heavy rainfall and flooding occurs more frequently on both sides of the tropical Pacific during periods of warmer Northern Hemisphere mean temperatures, implying that ENSO-driven rainfall extremes could intensify in the near future.

1. Introduction

1.1. Background

Changes in precipitation extremes constitute one of the largest threats to human well-being and are predicted to become more frequent due to anthropogenic climate change (Christensen et al., 2013). Floods and droughts can be particularly devastating in the tropics, where many societies lack the resilience to mitigate their impacts. Within the western tropical Pacific region, large-magnitude floods in Indonesia, including major floods in 2007–2008 and 2011–2012, have displaced hundreds of thousands of people and resulted in hundreds of deaths (Brakenridge, 2015). In Indonesia, precipitation extremes are often caused by the El Niño-Southern Oscillation (ENSO; Hendon, 2003), the dominant mode of tropical rainfall variability. Despite the impacts of precipitation extremes on Southeast Asian economies, and the importance of ENSO to the global climate system, it remains unclear how ENSO, western Pacific flooding, and drought have varied in the past and how they will vary in the future (Christensen et al., 2013; Vecchi and Wittenberg, 2010; Masson-Delmotte et al., 2013).

Existing reconstructions of ENSO and associated flooding over the last millennium are limited and mainly restricted to the central and eastern tropical Pacific. Flood records derived from lake sediment proxies in Ecuador (Moy et al., 2002) and the Galápagos (Conroy et al., 2008) exhibit substantial centennial-scale variability during the last millennium, suggesting El Niño-driven rainfall

* Corresponding author. U.S. Geological Survey, Florence Bascom Geoscience Center, 12201 Sunrise Valley Dr., MS926A, Reston, VA 20192, USA.
E-mail address: jrodysill@usgs.gov (J.R. Rodysill).

https://doi.org/10.1016/j.quascirev.2019.106020

decreased between ~1300 and ~1800 CE. However, the complex controls on flooding at these sites, and the lack of comparable records from the western Pacific, limits clear attribution of floods strictly to El Niño. Moreover, coral-based reconstructions of sea surface temperatures (SSTs) from the central Pacific Ocean lack evidence for ENSO variance changes in concert with eastern Pacific flooding (Cobb et al., 2013). Thus, the histories of ENSO and western tropical Pacific flooding are unresolved. In this study, we aim to illuminate the history of flooding in the western tropical Pacific over the last millennium to compare with existing eastern tropical Pacific flood reconstructions in order to assess the large-scale controls on extreme precipitation events in these two ENSO-sensitive regions.

1.2. Study site

To improve our understanding of ENSO and associated flooding in the western Pacific, we reconstructed the history of flooding in East Java, Indonesia using sedimentological data from Lake Lading (8.008833°S, 113.3125°E), a small, ~200 m diameter, 8.6 m deep lake. East Java is a heavily populated region where widespread agricultural practices have dramatically altered the landscape. Previous work in East Java has shown strong influences of these practices on sedimentation in East Javanese crater lakes (Rodysill et al., 2012). The catchment of Lake Lading is open forest and shrubland and is not currently cultivated, but the crater rim and adjacent areas are cultivated for coffee and other crops.

Rainfall near our study site averages 2560 mm/year (Vose et al., 1992), most of which occurs between November and April when the Australian-Indonesian Summer Monsoon strengthens and the Intertropical Convergence Zone (ITCZ) migrates southward. ENSO activity greatly influences interannual rainfall variability in East Java through changes to the Walker Circulation; El Niño events weaken atmospheric convection and cause drought, whereas La Niña events enhance convection and regional precipitation, driving heavy rainfall events (Hendon, 2003, Fig. 1). The relative influences of ENSO, the Walker Circulation, and the ITCZ on the Indonesian monsoon and rainfall are highly complex and not well understood, particularly over long timescales.

Lake Lading occupies a steep-sided maar crater composed of volcanic tuffs from the nearby Gunung Lamongan volcano. These sediments are rich in iron-bearing minerals that are easily detected by magnetic susceptibility (magsusc) measurements (Sandgren and Snowball, 2001). Heavy rainfall should intensify runoff and enhance the delivery of coarse sediments to the lake, such that exceptionally high magsusc and elevated coarse sediment contents should reflect flooding. Laminated sediments preserve individual beds of coarse sediments in our core (Rodysill et al., 2013, Fig. 2), and high sedimentation rates (0.4 cm/yr) allow for high-resolution analysis, making this record uniquely sensitive to anomalous precipitation events.

2. Methods

2.1. Instrumental precipitation data

To examine the relationship between precipitation at Lake Lading and large-scale atmospheric circulation patterns, we utilized local station rainfall data measured at the Randuagung weather station in East Java (8.07°S, 113.3°E), located ~15 km SE from our study site, obtained from the Global Historical Climatology Network and covering Jan. 1927 to Dec. 2011 (Vose et al., 1992). We calculated the seasonal rainfall standardized anomalies for December-January-February (DJF), March-April-May (MAM), June-July-August (JJA), and September-October-November (SON). We then tested the correlation between the seasonal rainfall standardized anomalies to seasonal Southern Oscillation Index (SOI; Ropelewski and Jones, 1987) values with a Pearson's R correlation from 1927 through 2011, with seasonal lags from 0 to 1 year.

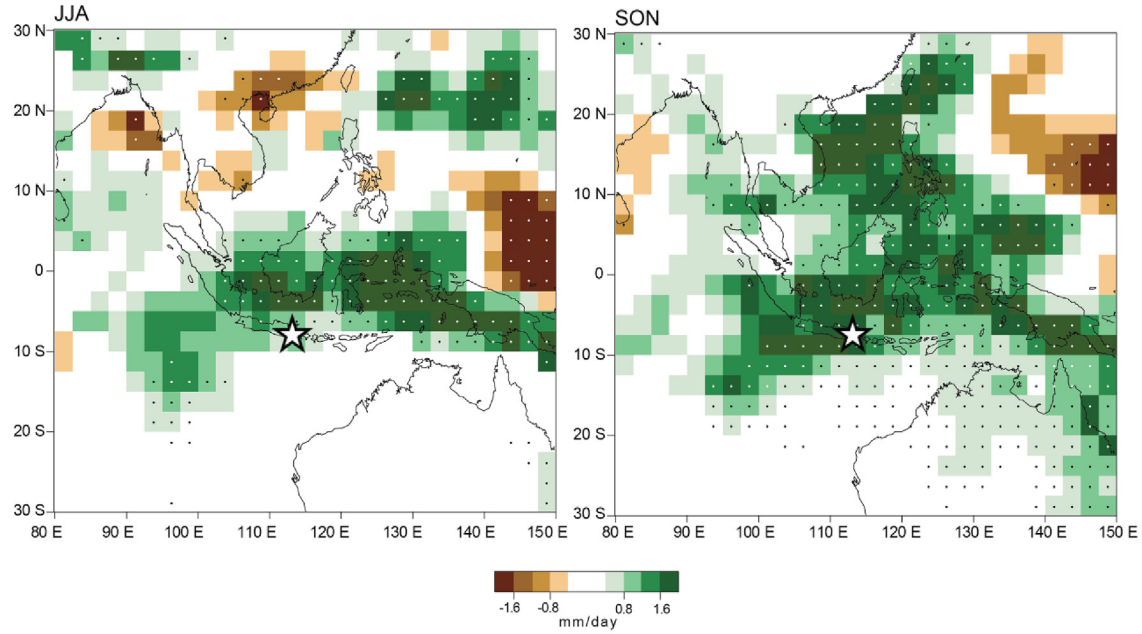

Fig. 1. La Niña precipitation anomalies at Lake Lading. Precipitation anomalies were calculated from GPCP Monthly Precipitation Analysis data (Adler et al., 2003) for June through August (left) and September through November (right) during La Niña years between 1979 and 2014, defined as a 5-month running mean SST value below −0.4 °C from the 1951–2000 mean in the Niño3.4 region for all 3 consecutive months in each season. La Niña years for June–August (left) include: 1984, 1985, 1988, 1989, 1999, 2000, and 2010; for September–November, La Niña years include: 1983, 1984, 1985, 1988, 1998, 1999, 2000, 2007, 2010, 2011. Stippled regions are statistically significant rainfall anomalies at the 95% level, determined from a two-tailed Student's t-test. Lake Lading is indicated by a star.

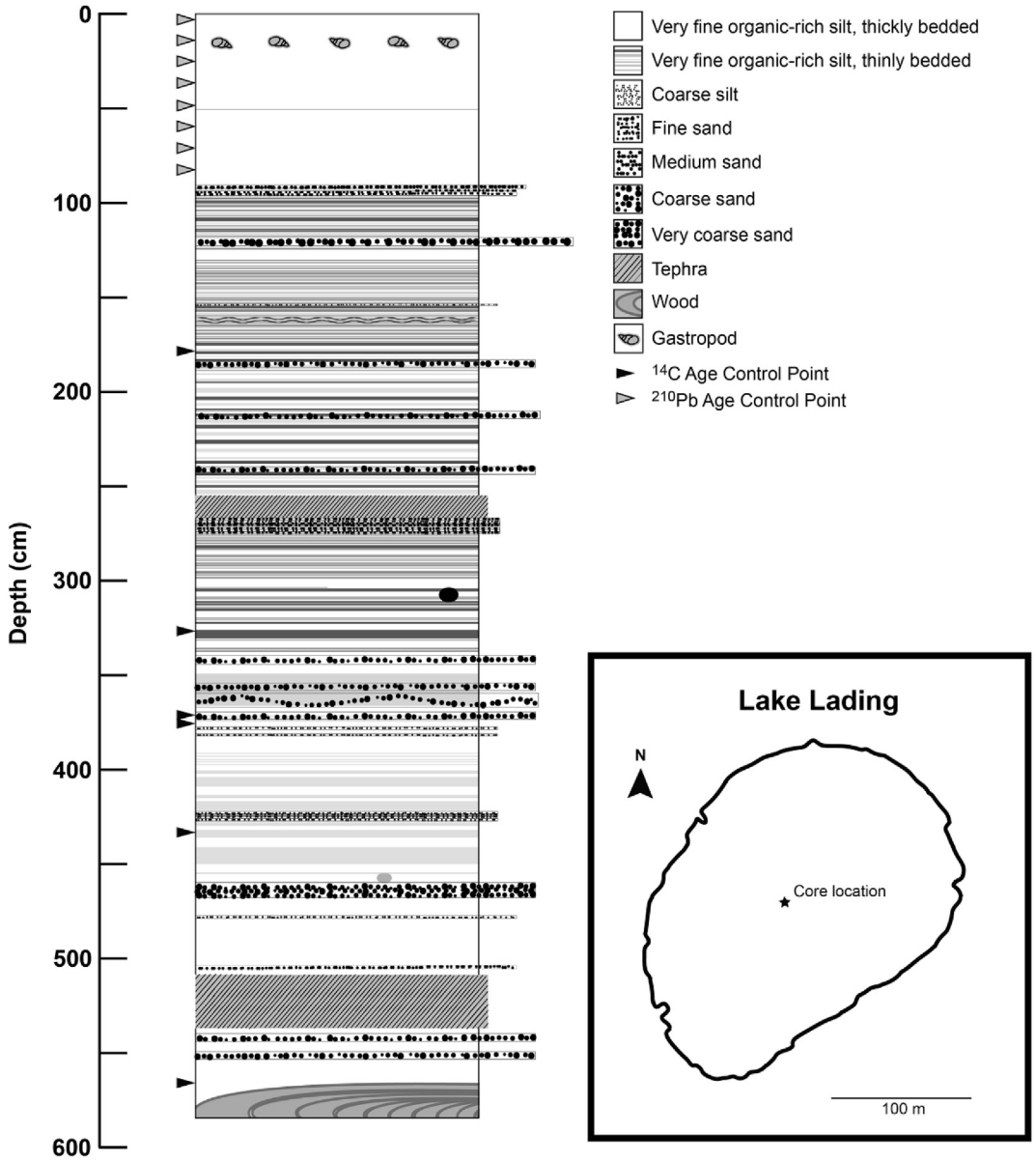

Fig. 2. Stratigraphic column of the Lake Lading sediment core versus depth. Lithologies are plotted with coarser sediments corresponding to wider stratigraphic units in the column. Age control points are indicated by triangles along the left side of the stratigraphic column. The composite core from Lake Lading consists of thin beds of diatom oozes alternating with thin beds of silts and sands. The sediments are very thinly bedded from 570 cm to 90 cm depth, above which the sediments become thickly-bedded to massive. Two tephra beds at 940 and 1600 CE were removed from the composite stratigraphy prior to application of the age model. The inset is a map displaying the core location within Lake Lading.

2.2. Lacustrine sedimentologic data

The 570 cm-long composite sediment core is derived from two overlapping cores collected in July 2008 from the deepest water near the center of the lake using a Bolivia corer above 2.5 m and a Livingstone corer below 2.5 m (Fig. 2). The upper 12 cm of the composite section was collected with a Uwitec gravity corer in 2008 and in 2010; surface sediments were extruded in the field in 1-cm increments. We measured magsusc at 1-cm resolution using a point sensor meter on a GeoTek Multi-Sensor Corelogger. To determine coarse sediment (% sand) content, the sediments were sampled in continuous 1-cm increments, and each sample was combusted for loss-on-ignition (LOI) following the protocol of Dean (1974), sieved at 63 μm, and dried at 100 °C overnight. We optically examined a subset of combusted samples to verify that sediment particles were not fused into secondary coarse particles during the combustion process.

Our prior work in a nearby crater lake, Lake Logung (Rodysill et al., 2012), documented a 4‰ enrichment in the nitrogen isotopic composition of organic matter ($\delta^{15}N_{org}$) circa 1860 CE that coincides with intensification of agricultural activity in East Java (Poesponegoro and Notosusanto, 1984). To examine the timing of land-use change and its impacts on Lake Lading sedimentary succession, sediment sub-samples were taken at ~7.5 cm resolution for nitrogen isotopic analysis and were pretreated to remove inorganic forms of N by soaking in 1 N HCl at room temperature for 1 h. The samples were rinsed five times with ultra-pure deionized water, and then dried and homogenized for analysis on a Costech Instruments elemental combustion system coupled to a Delta V Plus isotope ratio mass spectrometer with a Conflo II interface. The standard deviation of the $\delta^{15}N_{org}$ standards was 0.256‰. A subset of samples was measured prior to and after pretreatment to

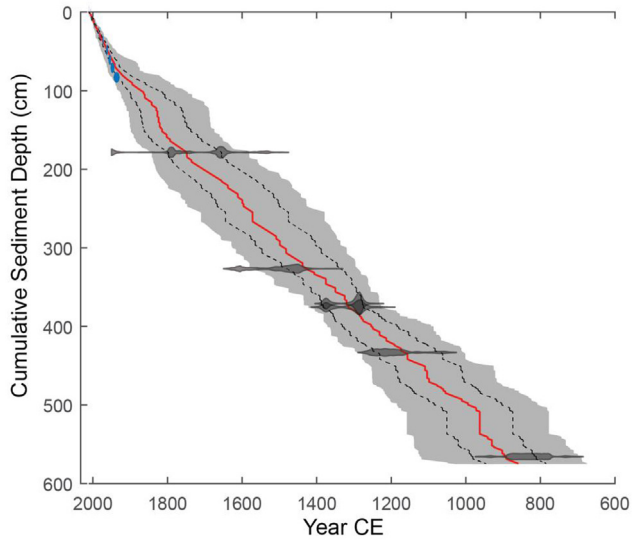

Fig. 3. The Lake Lading age model. The weighted mean age-depth relationship is shown in red, the 95% uncertainty bounds are shown by dashed lines, and the gray shading highlights the full range of age models produced by Bacon (Blaauw and Christen, 2011). Calibrated radiocarbon ages and associated probability distributions are displayed as dark gray horizontal shapes, and core-top ages derived from ^{210}Pb ages are displayed as blue diamonds. (For interpretation of the references to color in this figure legend, the reader is referred to the Web version of this article.)

determine the effects of acidification on $\delta^{15}N_{org}$ values, which revealed that the isotopic values of both sets of samples were well within our analytical precision with no bias between acidified and unacidified samples.

The chronology of Lake Lading sediments is based upon six ^{14}C ages determined from plant macrofossils and a ^{210}Pb constant rate of supply model, detailed in Rodysill et al. (2013). We revised the age-depth relationship to account for deposition of sand beds, which we interpret to reflect short-lived flood events. To isolate the major flood deposits from lower-amplitude runoff events and other variations in sediment input, we assumed an average sedimentation rate of 0.45 cm/yr based on the original age model described in Rodysill et al. (2013) and applied a 12th order high-pass filter with a 10-year cutoff frequency to the % sand and magsusc. This filter best captured the centimeter-scale sand beds characteristic of event deposition. The trends identified in these data are robust across a range of high-pass filters and other filtering methods (e.g. first-difference). The filter identified fifty visually-distinct sand beds and two decimeter-scale tephra beds, which were removed from the depth scale prior to age model development. We calculated the age-depth relationship using Bacon v. 2.2 (Blaauw and Christen, 2011, Fig. 3) and subsequently reinserted the coarse beds into the stratigraphy to calculate their age.

To differentiate intensified sand deposition due to floods from lower amplitude runoff deposits that occur during typical wet season rains, flood deposits are defined as sand beds that are coarser than 80% of the high-pass filtered dataset. Our interpretations are based on trends common to both the high-pass filtered dataset and the unfiltered % sand dataset. We used change point analysis to identify the 5 most significant change points in both the % sand and flood presence/absence time series. Other statistical analyses of the data are described below.

3. Results

3.1. ENSO, precipitation, and flood relationships

Local precipitation at Randuagung is positively, significantly correlated ($p < 0.001$) to the SOI in austral spring and winter (JJA and SON) with the strongest correlations at zero lag (Table 1). These results are consistent with seasonal composite data indicating positive rainfall anomalies occur in East Java during the austral winter and spring of La Niña years (Fig. 1) and a stronger correlation between Indonesian rainfall and Pacific Ocean SSTs during JJA and SON (Hendon, 2003).

The historic flood record from East Java is derived from news reports (Brakenridge, 2015) and is likely incomplete, limiting quantitative analyses of the relationship between regional flooding and local rainfall during and between La Niña events. However, of the 17 floods occurring across East Java between 1985 and 2010, 14 floods (82%) coincided with anomalously positive monthly precipitation values at Randuagung. This observation suggests that heavy rainfall and flooding across East Java tends to coincide with heavy rainfall near our study site. Furthermore, 11 of these floods (65%) occurred during months characterized by positive SOI values, suggesting clear links between ENSO activity and flooding at our study site.

Because instrumental flood records are not available for this part of Java, we also analyzed output from the Community Earth System Model-Last Millennium Ensemble (CESM-LME) control simulation (Otto-Bliesner et al., 2016) to test the extent to which modeled runoff in East Java was correlated to ENSO variability during the past millennium. Annually-averaged CESM-LME precipitation and runoff anomalies in East Java are negatively correlated to annually-averaged Niño 3.4-index anomalies ($R = -0.76$ and -0.62, respectively; $p < 0.001$) between 850 and 2005 CE (Fig. 4). Greater than 80% of simulated La Niña years, defined as a negative departure greater than one standard deviation below the annually-averaged Niño 3.4-index mean of the CESM-LME control simulation, corresponded to positive anomalies in the annually-averaged runoff data from the model grid points containing Lake Lading (latitude = −6.4 to −8.8, longitude = 108.5 to 114.5). Runoff values exceeding one standard deviation from the mean, calculated between 850 and

Table 1
Precipitation and Southern Oscillation Index correlations. Correlations between East Java rainfall and the Southern Oscillation Index (SOI) are listed in this table for: December-January-February (DJF), March-April-May (MAM), June-July-August (JJA), and September-October-November (SON). We performed lagged correlation analyses between the SOI and rainfall in the same season and each subsequent season in the rainfall dataset for one full year. Correlations significant at the 95% level are underlined, and correlations significant at the 99.9% level are in bold.

East Java Precipitation Seasons									
Index Seasons		Year 0				Year +1			
		DJF	MAM	JJA	SON	DJF	MAM	JJA	SON
SOI	DJF	−0.055	−0.154	−0.039	−0.301	−0.129			
	MAM		0.039	0.173	0.146	−0.281	−0.180		
	JJA			**0.451**	**0.518**	−0.168	−0.284	−0.046	
	SON				**0.613**	−0.156	−0.220	−0.083	−0.255

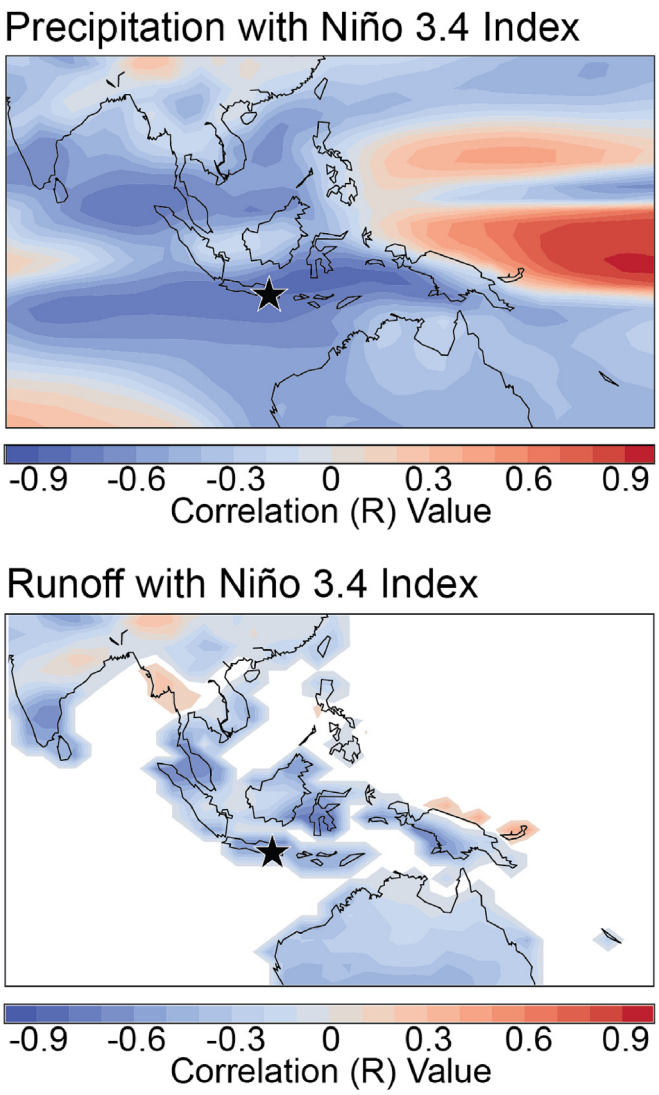

Fig. 4. Modeled correlations between precipitation, flooding and ENSO index. Correlations between the reconstructed Niño 3.4 index, precipitation, and runoff at Lake Lading in the Community Earth System Model-Last Millennium Ensemble (CESM-LME) control simulation dataset for the past millennium (Otto-Bliesner et al., 2016).

2005 CE, reflect anomalously high simulated runoff as would occur during flood years. Years characterized by a positive runoff anomaly occurred three times more often during La Niña years than during non-La Niña years. The strong, highly significant correlations between precipitation, runoff anomalies, and the Niño 3.4-index suggest that Pacific Ocean dynamics have been the principal driver of flooding in East Java during the past millennium.

3.2. Historic sedimentation in Lake Lading

The $\delta^{15}N_{org}$ data from Lake Lading can provide insight into when human activity in the catchment began to influence sedimentation, as is the case at nearby Lake Logung (Rodysill et al., 2012). $\delta^{15}N_{org}$ values averaged 0.45‰ from ~850 to 2010 CE (Fig. 5). A 4.5‰ enrichment in $\delta^{15}N_{org}$ between 1825 and 1850 CE in Lake Lading, similar to the signal in Lake Logung, coincides with regional agricultural intensification, and likely indicates lake eutrophication. Between 1900 and 2010 there is a return to more depleted isotopic values from ~4‰ to 1‰, but present-day values remain enriched by ~1‰ relative to the $\delta^{15}N_{org}$ prior to the mid-1800s. This is associated with large changes in landscape erosion rates. Sedimentation rates, grain size, and magsusc rose rapidly during the early 1800's, coincident with $\delta^{15}N_{org}$ enrichment, indicating that recent sedimentation is strongly influenced by human activities and landscape disturbance. This shift is also marked by a transition from thinly to thickly bedded to massive sediments, which severely limits our ability to detect coarse sediment layers during the most recent two centuries. Because of these anthropogenic impacts on Lading sedimentation, we excluded the core-top sediments (after ~1825 CE) from our flood analyses.

3.3. Reconstructed flood time series

We detect 50 major floods in the Lake Lading record. Filtered magsusc maxima (exceeding ~200 SI) align with 92% of filtered % sand anomalies (exceeding ~20%), indicating that both proxies record the same events. Our record indicates that floods were more frequent prior to ~1300 CE and less frequent from ~1400 CE until just prior to the onset of agricultural intensification about 1800 CE (Fig. 5). A Mann-Whitney difference of means test computed for the intervals 900 to 1250 CE and 1400 to 1850 CE reveals that the % sand median is significantly different between these time intervals at the 5% significance level. We detected a significant change point in both the % sand and flood presence/absence time series in the mid-late 1300s (Table 2), indicating the shift in flood regime is statistically robust (at the 5% significance level). The significant reduction in unfiltered % sand during the 14th century demonstrates that detection of this regime shift is insensitive to the methods used for identifying flood deposits. Repeated change point detection of the % sand time series across a suite of 1000 age model realizations places the timing of the regime shift between 1260 and 1480 CE, with the most probable timing centered on 1400–1410 CE.

4. Discussion

4.1. Controls on sand deposition in Lake Lading

Floods resulting from heavy rainfall at Lake Lading should deliver anomalously coarse sediments from the landscape into the lake and generate high magsusc values. However, other processes can result in deposition of sand near the center of the lake basin, such as changes in the flow of river inputs, earthquakes, shoreline migration during lake lowstands, or, as described above, human impacts. Lake Lading has no river or stream inflows, and instead receives much of its clastic inputs from surface runoff. The coarse beds in Lake Lading sediments lack characteristics that are commonly associated with earthquake-driven deposition, including sediment debris flows and microfaults (Beck et al., 1996). If lake lowstands were responsible for the deposition of coarse deposits observed in our cores, we would expect that intervals of prolonged drought would correlate to intervals with coarser sediments in Lake Lading. However, a comparison of centennial-scale drought reconstructions from Lake Lading and nearby Lake Logung reveals that droughts correspond to low coarse content and magsusc (Rodysill et al., 2013; Rodysill et al., 2012, Fig. 5). For instance, the most intense drought in the Lake Lading record is marked by an interval of calcium carbonate deposition between 1790 and 1860 CE, recorded by Ca:Ti, and coincides with a lull in coarse sediment deposition (Rodysill et al., 2013, Fig. 5) and a significant regime shift toward fewer floods just prior to 1800 CE (Table 2).

A significant regime shift ~1815 CE (Table 2) toward very high percent sand values (exceeding 60%) and up to 6 floods per 50-year window, preceding evidence for anthropogenic activities within the catchment, likely reflects flooding in Lake Lading that is driven

by an increase in precipitation following prolonged drought in East Java (Vose et al., 1992, Fig. 5). We interpret the increase in flood deposits prior to ~1825 CE as intensified rainfall and runoff at Lake Lading, noting that the severe drought could have destabilized the landscape and amplified the climate signal in the sediment record. Decadal periods of depleted δD (wet) measured on the same sediment core (Konecky et al., 2013, Fig. 5) occur when sand content and magsusc in Lake Lading indicate runoff was high, supporting our interpretation that coarse deposits and higher magsusc are associated with wet conditions. Interestingly, the multicentennial-scale trends in flood occurrence appear to be unrelated to the millennium-long increase in rainfall inferred from the δD dataset, implying that these proxies may be sensitive to different elements of the hydrologic cycle, and the mechanism driving floods differs from that driving low-frequency precipitation changes.

Extensive land clearance and agriculture beginning in the mid-1800s strongly affected Lake Lading and its sediment. After ~1825 CE, a significant regime shift toward increases in % sand and flood occurrence (Table 2) coincides with $\delta^{15}N_{org}$ enrichment and appears to be mainly driven by anthropogenic activities (Fig. 5). Moreover, the gradual decline in grain size and magnetic susceptibility after 1900 CE are unlikely to reflect a reduction in runoff intensity due to a drying climate, because there has not been substantial drying between 1927 and present in nearby station rainfall data (Vose et al., 1992). Rather, these changes likely reflect the effects of lake eutrophication, which accelerates sedimentation rates, and landscape re-stabilization following agricultural clearance. These observations and evidence for severely altered nitrogen cycling indicate that catchment activities strongly influenced the sediment record, leading us to omit the period 1825 to 2010 CE from the flood reconstruction.

4.2. La Niña-driven flooding at Lake Lading

We lack observational records of surface runoff and flooding, such that we cannot directly compare the sedimentary record of flooding during the last century to instrumental rainfall records to calibrate the Lake Lading record. However, rainfall measured at a nearby weather station in East Java is strongly positively correlated ($p < 0.001$) to the SOI, and model simulations spanning the last millennium indicate precipitation and runoff anomalies in East Java are negatively correlated (−0.76 and −0.62, respectively; $p < 0.001$) to modeled Niño 3.4-index anomalies (Fig. 4). Historically, floods across East Java occur during periods of regionally heavy rainfall and tend to coincide with La Niña anomalies. These results implicate La Niña as a source of increased rainfall and flooding in East Java and as an important control on flood deposits in our record.

Floods in East Java are short-duration (hours to weeks) events, and multiple, closely-spaced flood deposits would not be distinguishable in the 1-cm (~1–3 year) sampling resolution of the Lake Lading sediments. Thus, although our record captures a 1–3 year average of flooding episodes in East Java, it does not provide a complete history of individual floods occurring on sub-annual time-scales. Due to the limitations of our age model, our record cannot link individual ENSO events in the eastern and western Pacific and therefore cannot discern the spatial patterns in precipitation necessary to document "flavors" of ENSO, such as La Niña Modoki (Ashok et al., 2007). El Niño events producing precipitation anomalies concentrated in the central Pacific (e.g. El Niño Modoki) have little difference in their effects on East Javan rainfall from events in the far east; our flood reconstruction is not able to distinguish between the different flavors of ENSO, or really to detect El Niño events in general. Further, while La Niña generates conditions that may lead to local flooding, not all La Niña events trigger flooding at our study site, and flooding can result from other climate phenomena. Thus, the record of flooding at Lake Lading, or any other site for that matter, provides an incomplete record of La Niña and ENSO variability. Nevertheless, the unique sensitivity of our sedimentary record to flooding, combined with the strong relationship between precipitation, runoff, and La Niña events in East Java supports our interpretation that this record captures floods that are likely to occur in the context of La Niña, providing insight into precipitation extremes and ENSO variability during the past millennium.

4.3. Lake Lading flood reconstruction in the context of tropical paleoclimate

The shift in flood regimes in eastern Indonesia at ~1400 CE is remarkably similar to the timing of changes in average northern hemisphere temperature (Andersen et al., 2004; Ljungqvist, 2010), with frequent Indonesian flooding during the warm Medieval Climate Anomaly (MCA), followed by less frequent flooding during the cool Little Ice Age (LIA). We iteratively computed Pearson's R correlation values for lowpass-smoothed flood and temperature datasets across a suite of 1000 Lake Lading age models and isolated the median (R_{med}) and maximum (R_{max}) R values. The flood time series is positively correlated to mean Northern Hemisphere temperature reconstructed from the NGRIP ice core (Andersen et al., 2004) at the 50-year ($R_{med} = 0.14$) and 100-year ($R_{med} = 0.24$) timescales ($p < 0.001$) and mean temperature reconstructed from synthesized continental temperature records (Ljungqvist, 2010) at the 100-year timescale ($R_{med} = 0.18$, $p < 0.05$; $R_{max} = 0.48$, $p < 0.05$).

Numerous lines of evidence suggest that the ITCZ migrated northward during the MCA and southward during the LIA (Sachs et al., 2009; Wang et al., 2005; Zhang et al., 2008; Richey and Sachs, 2016). However, our data suggest that floods were less common during the LIA and more common prior to and after the LIA (Fig. 5). Although recent syntheses suggest that the tropical rain belt could have contracted, rather that migrated southward, during the LIA (Yan et al., 2015), local data indicate that East Java was generally wetter during the LIA than during the MCA (Konecky et al., 2013; Rodysill et al., 2012), in keeping with theory linking ITCZ migration to changes in the interhemispheric temperature gradient (Broccoli et al., 2006). Thus, our record indicates that changes in flood frequency cannot be explained by long-term, meridional shifts in the mean position of the tropical rain belt.

Lake sediment archives from the Galápagos Islands (Conroy et al., 2008) and Ecuador (Moy et al., 2002) indicate a statistically robust decrease in flood frequency in the eastern tropical Pacific circa 1300–1400 CE, synchronous (within age model uncertainty) with decreased flood frequency in East Java (Fig. 6; Table 2). We iteratively computed Pearson's R correlation values for 50-year lowpass-smoothed flood datasets across a suite of 1000 Lake Lading age models and isolated the median (R_{med}) and maximum (R_{max}) R values. Flood frequency at the 50-year timescale in East Java is significantly, positively correlated with flood variability in the Galápagos Islands ($R_{med} = 0.09$, $p < 0.05$ and $R_{max} = 0.59$, $p < 0.05$) and with flood frequency in Ecuador ($R_{med} = 0.40$, $p < 0.05$ and $R_{max} = 0.68$, $p < 0.05$). These eastern Pacific records have been interpreted to reflect changes in the frequency of El Niño events, due to the relationships between eastern Pacific SST anomalies and regional precipitation. Moreover, the flooding recorded in Laguna Pallcacocha, Ecuador occurs within the ENSO frequency band (Moy et al., 2002; Schneider et al., 2018). Indeed, the Pallcacocha record has often been used as a benchmark record of ENSO variability; however, analyses of instrumental data indicate that regional precipitation anomalies in the Andes can arise from diverse mechanisms (Schneider et al., 2018), calling into question the use of these

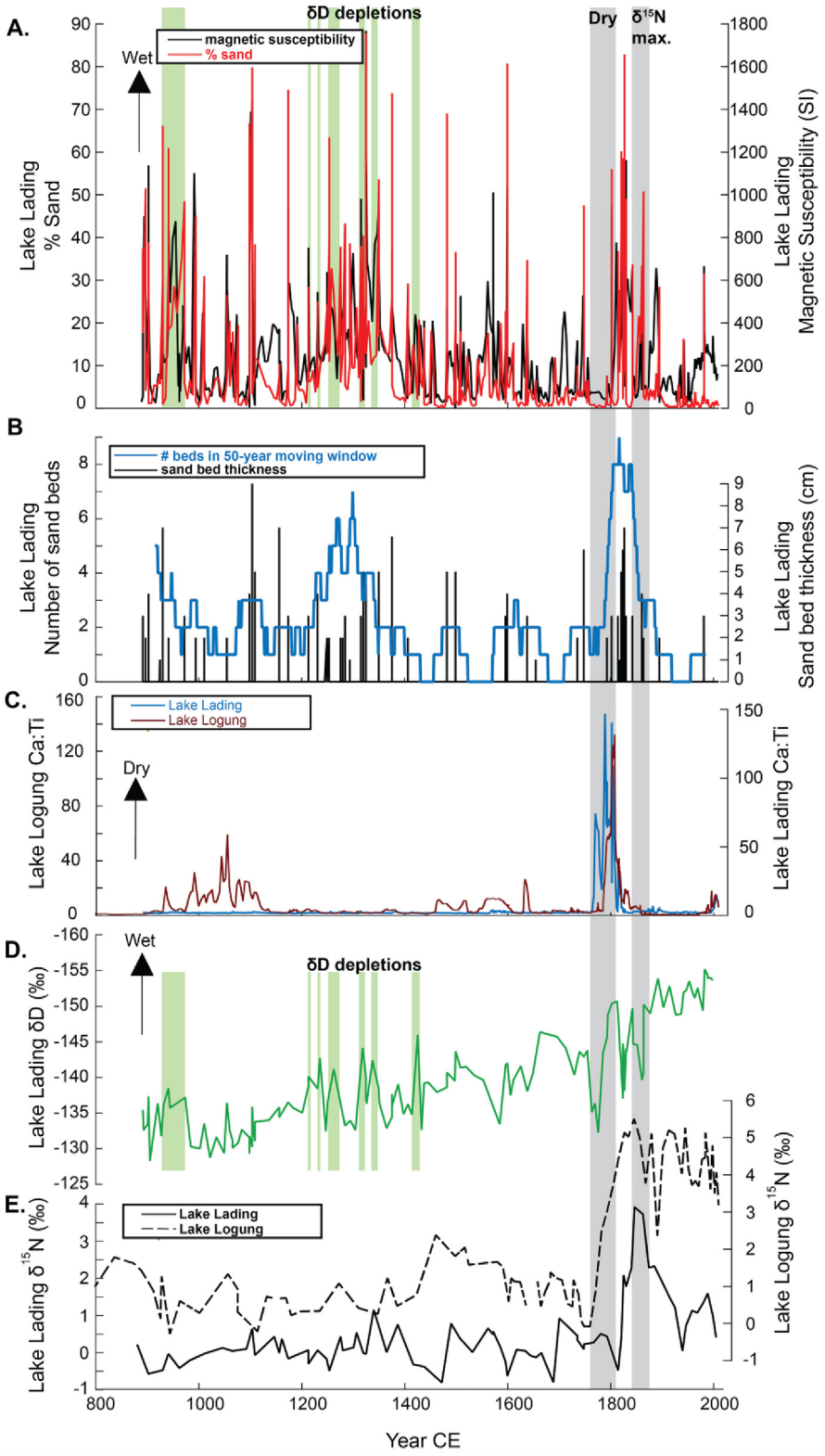

Fig. 5. Lake Lading limnologic data. (A) Magsusc (black; right axis) and % sand (red; left axis). (B) Sand bed thickness in cm (black, right axis) and the number of sand beds in a 50-yr sliding window (blue, left axis). (C) Ca:Ti-based carbonate abundance records from lakes Lading (blue; right axis; Rodysill et al., 2013) and Logung (maroon; left axis; Rodysill et al., 2012), plotted such that higher carbonate, interpreted as drought, is up. (D) δD from Lake Lading sediments is plotted in per mille with more depleted values (wet) up (green; Konecky et al., 2013). (E) The nitrogen isotopic composition of sedimentary organic matter ($\delta^{15}N_{org}$) from Lake Lading (solid line) and Lake Logung (dashed line; Rodysill et al., 2012). Values are reported relative to atmospheric $\delta^{15}N$ in per mille. Gray vertical shading highlights a period of prolonged East Java drought (Rodysill et al., 2013) and the nitrogen isotopic maxima in the Lake Lading record. Green vertical shading in A and D are deuterium isotopic minima in the Lake Lading record. All datasets are plotted versus Year CE.

Table 2
Regime shift detection in flood records. Regime shift detection tests performed using change point detection methods are listed in this table for the % sand and flood presence/absence datasets from Lake Lading, the red color intensity data from Laguna Pallcacocha (Moy et al., 2002), and the % sand dataset from El Junco Lake (Conroy et al., 2008). The top five significant (at the 95% level) change points in each time series during the period of overlap (~900–2000 CE) are listed as years in the Common Era (CE). Bolded values highlight the regime shift occurring during the MCA-LIA transition and are discussed in the text. Italicized values highlight the regime shifts that are interpreted to reflect land-use change in Lake Lading sediments and are thus not discussed in terms of variability in climate and flood occurrence.

	Lake Lading % Sand	Lake Lading Flood Presence/Absence	Laguna Pallcacocha Red Color Intensity	El Junco Lake % Sand
Change Point 1	*1830 CE*	*1889 CE*	1609 CE	1987 CE
Change Point 2	1815 CE	*1848 CE*	1593 CE	1951 CE
Change Point 3	**1375 CE**	1795 CE	**1337 CE**	1858 CE
Change Point 4	1104 CE	**1344 CE**	**1334 CE**	**1278 CE**
Change Point 5	1099 CE	1228 CE	992 CE	1018 CE

records to reconstruct ENSO.

What might cause extreme precipitation events to covary on opposite sides of the tropical Pacific? Multiple mechanisms, including changes in monsoon strength and/or tropical cyclone activity, can drive heavy rainfall in these regions, but the reconstructed patterns of floods are not easily explained by these drivers. It is unlikely that tropical cyclones would trigger simultaneous shifts in rainfall variability on both sides of the tropical Pacific Ocean. As already noted, a northward shift in the mean position of the ITCZ could decrease rainfall, and thus flooding, at all three sites; however, theory and proxy evidence indicate the ITCZ contracted and/or shifted southward, toward these southern tropical sites, across the MCA to LIA transition (Rodysill et al., 2012; Sachs et al., 2009; Wang et al., 2005; Zhang et al., 2008; Richey and Sachs, 2016).

Rather, we argue that the correlation in flood patterns between the eastern and western Pacific reflects ENSO-driven precipitation variability during the last millennium. Extreme precipitation at our site is often linked to La Niña events, and we infer that La Niña was intensified during the MCA. A record from Bainbridge Crater Lake in the Galápagos also supports a shift from more frequent La Niña events during the MCA to reduced La Niña activity during the LIA (Fig. 6; Thompson et al., 2017). That records from both the eastern and western Pacific, ENSO's two main centers of action, show a shift from frequent flooding to less frequent flooding circa 1300–1400 CE implies that ENSO-driven precipitation variability – both El Niño and La Niña – intensified during the MCA and weakened during the LIA. ENSO events are inherently ocean temperature phenomena, and changes in precipitation, often driven by changes in the east-west atmospheric Walker Circulation, are not a direct measure of ENSO variability. Biomarker-based reconstructions from the Peru Margin indicate a coherent increase in El Niño and La Niña activities during the MCA (Makou et al., 2010) at a time when coral-based reconstructions of tropical Pacific SSTs and ENSO are temporally sparse (Cobb et al., 2013). Our data thus show that El Niño- and La Niña-driven rainfall anomalies co-varied on multi-centennial timescales.

The observation that La Niña-driven flooding decreased near the end of the MCA and beginning of the LIA suggests links between ENSO activity and large-scale temperature changes. One mechanism linking warmer temperatures and to more extreme ENSO events that is particularly relevant to future warm climates relates to SST warming that occurs at a higher rate in the eastern equatorial Pacific relative to the western equatorial Pacific and the northern tropical eastern Pacific (Cai et al., 2014, 2015). In climate model simulations, a reduction in zonal and meridional SST gradients leads to atmospheric convection anomalies in the eastern equatorial Pacific and a weakening of the atmospheric Walker Circulation; deep atmospheric convection in the eastern equatorial Pacific occurs in the model with smaller SST anomaly perturbations during warmer periods. Although a more northerly mean ITCZ during the MCA would appear to contradict the formation of more extreme ENSO events, which rely on low level convergence characteristic of the ITCZ to be drawn over the equator (Cane, 2005), the model output shows that a higher rate of warming in the eastern equatorial Pacific relative to the northerly climatological position of the ITCZ can induce atmospheric convection necessary for El Niño anomalies to grow (Cai et al., 2014). These dynamical changes lead to more frequent strong El Niño events in the model, which set the stage for strong La Niña events as warm surface waters shift westward, the thermocline shoals, and cooler SSTs in the central Pacific lead to intensified easterlies after the strong El Niño event breaks down (Cai et al., 2015). Strong La Niña events also occur more often in a warmer climate in the model by enhancing sensitivities of feedbacks; smaller magnitude SST cooling in the central Pacific following El Niño events can trigger the Bjerknes feedback relative to a cooler climate (Cai et al., 2015).

A similar mechanism may have led to intensified ENSO events and associated rainfall anomalies in Indonesia and the eastern Pacific during the MCA relative to the LIA, although radiative forcing differed relative to the forward-looking anthropogenically-forced model simulations, and the relationships between the mean state and variability of the tropical Pacific are still debated (Christensen et al., 2013; Vecchi and Wittenberg, 2010; Cai et al., 2014, 2015; Cane, 2005; Stevenson et al., 2017). Paleotemperature data from the eastern Pacific indicate that the zonal SST gradient was weaker during the peak MCA northern hemisphere warmth (Rustic et al., 2015) than during the LIA, and some hydrology reconstructions suggest the Walker Circulation weakened during the MCA. For example, centennial-resolution records from the southern Indo-Pacific Warm Pool (IPWP) region indicate the MCA (LIA) was dry (wet), on average (Oppo et al., 2009; Tierney et al., 2010; Rodysill et al., 2012; Konecky et al., 2013) when mean runoff was high (low) in the east (Conroy et al., 2008), implying convection was reduced in the west and enhanced in the east during the MCA relative to the LIA. Our reconstruction of increased La Niña-driven rainfall anomalies coinciding with increased El Niño-driven rainfall frequency during the MCA relative to the LIA is consistent with warmer Northern Hemisphere temperatures and evidence for a weaker Walker Circulation and zonal SST gradient inferred from hydrologic and SST records.

5. Conclusions

Controls on ENSO variability on long timescales are debated. Although some studies suggest ENSO may respond to natural and anthropogenic radiative forcing (Cane, 2005; Stevenson et al., 2017; Clement et al., 1996), stochastic processes can drive large, unforced variations in ENSO (Rustic et al., 2015; Cobb et al., 2013) that can overwhelm forced variability. Nevertheless, our data document a clear shift in flood regimes that coincided with changes in northern hemisphere temperature during the last millennium. The similarity

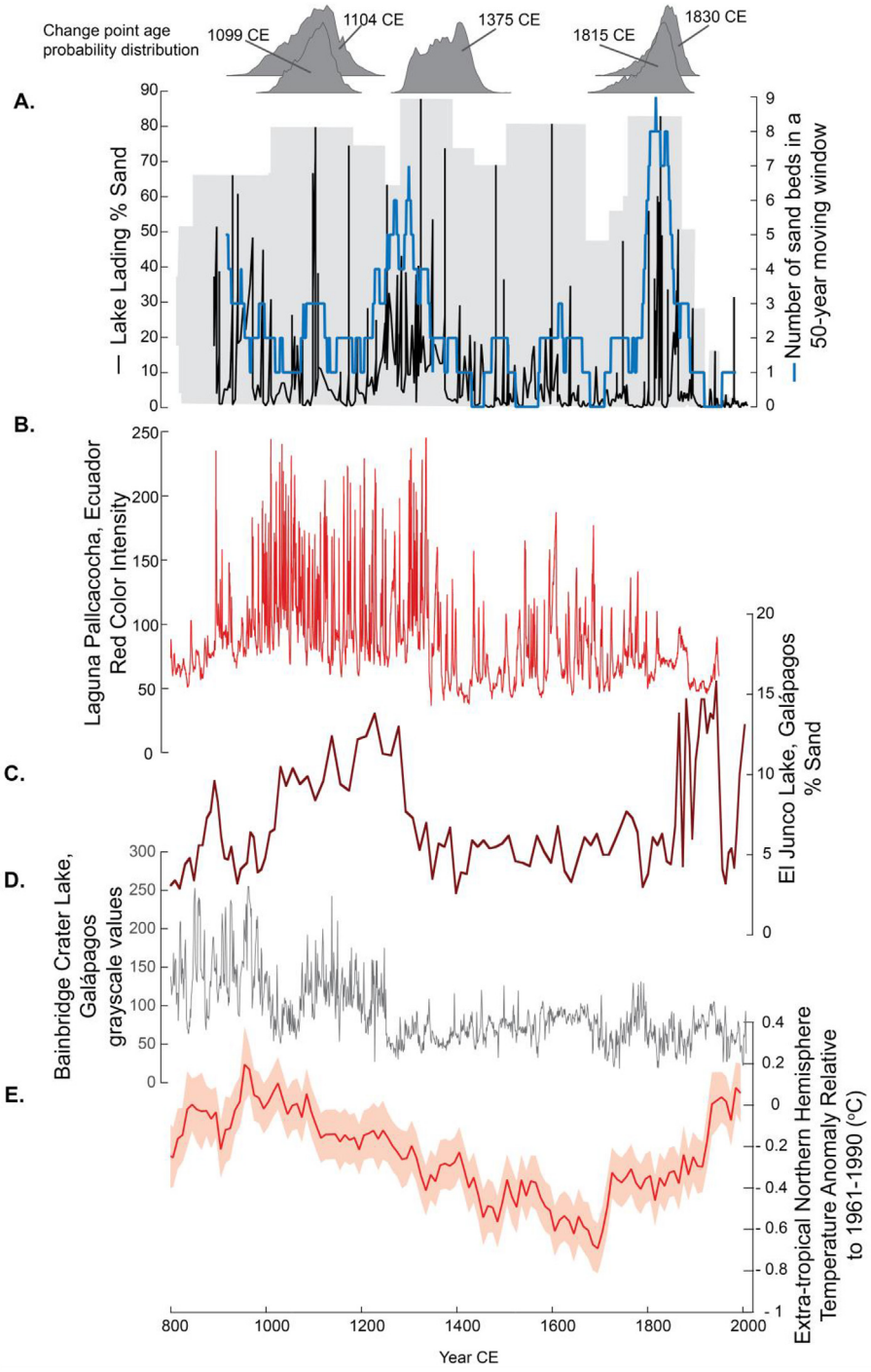

Fig. 6. Comparison of Lake Lading flood record with tropical Pacific and Northern Hemisphere climate reconstructions. The Lake Lading flood record, eastern equatorial Pacific flood records, Galápagos drought record, and mean Northern Hemisphere reconstructed temperature are plotted versus Years CE. Histograms at the top of the figure displays the Bacon-derived age probabilities for the five change points identified in the Lake Lading % sand data, which are listed in Table 2. (A) Lake Lading % sand (black, left axis) and number of sand beds in a 50-year moving window (blue, right axis). Gray shading represents age model uncertainty on the % sand dataset. (B) Red color intensity from Laguna Pallcacocha, Ecuador (Moy et al., 2002). (C) % sand from El Junco Lake, Galápagos (Conroy et al., 2008). (D) Grayscale data from Bainbridge Crater Lake, Galápagos (Thompson et al., 2017) interpreted such that higher values indicate drier conditions associated with La Niña activity. (E) Northern Hemisphere reconstructed mean temperature (Ljungqvist, 2010). Light red shading represents reconstructed temperature uncertainty. (For interpretation of the references to color in this figure legend, the reader is referred to the Web version of this article.)

between our new flood reconstruction from the western Pacific and flood records from the eastern Pacific implicate ENSO variability as the control on this regime shift, thus indicating increased ENSO variability during periods of increased radiative forcing and northern hemisphere warming during the last millennium. Although our record cannot constrain recent shifts in the ENSO system and future radiative forcing differs from that of the MCA, our results support climate model predictions that the future could hold more intense, ENSO-driven heavy precipitation events in the tropics (Christensen et al., 2013; Cai et al., 2014, 2015), with potentially serious implications for populations in and near the tropical Pacific Ocean.

Acknowledgements

We thank the Government of the Republic of Indonesia and the Ministry of Research, Technology, and Higher Education (RISTEK) for permission and assistance in conducting field research. We thank Candace Bousquet for laboratory assistance, Baylor Fox-Kemper for helpful discussions, and Tom Cronin and two anonymous reviewers for improving the quality of this manuscript. This material is based upon work supported by the US National Science Foundation [grant number 0902845], the National Geographic Society [grant number 8083-06], and the National Oceanic and Atmospheric Administration Climate Change Data and Detection program [grant number NA09OAR4310090]. Any use of trade, product or firm names is for descriptive purposes only and does not imply endorsement by the U.S. government.

References

Adler, R.F., Huffman, G.J., Chang, A., Ferraro, R., Xie, P.-P., Janowiak, J., Rudolf, B., Schneider, U., Curtis, S., Bolvin, D., Gruber, A., Susskind, J., Arkin, P., Nelkin, E., 2003. The version 2 global precipitation Climatology project (GPCP) monthly precipitation analysis (1979-present). J. Hydrometeorol. 4, 1147–1167. https://doi.org/10.1175/1525-7541(2003)004<1147:TVGPCP>2.0.CO;2.

Andersen, K.K., Azuma, N., Barnola, J.-M., Bigler, M., Biscaye, P., Caillon, N., Chappellaz, J., Clausen, H.B., Dahl-Jensen, D., Fischer, H., Flückiger, J., Fritzsche, D., Fujii, Y., Goto-Azuma, K., Grønvold, K., Gundestrup, N.S., Hansson, M., Huber, C., Hvidberg, C.S., Johnsen, S.J., Jonsell, U., Jouzel, J., Kipfstuhl, S., Landais, A., Leuenberger, M., Lorrain, R., Masson-Delmotte, V., Miller, H., Motoyama, H., Narita, H., Popp, T., Rasmussen, S.O., Raynaud, D., Rothlisberger, R., Ruth, U., Samyn, D., Schwander, J., Shoji, H., Siggard-Andersen, M.-L., Steffensen, J.P., Stocker, T., Sveinbjörnsdóttir, A.E., Svensson, A., Takata, M., Tison, J.-L., Thorsteinsson, Th., Watanabe, O., Wilhelms, F., White, J.W.C., 2004. High-resolution record of Northern Hemisphere climate extending into the last interglacial period. Nature 431, 147–151. https://doi.org/10.1038/nature02805.

Ashok, K., Behera, K.S., Rao, S.A., Weng, H., Yamagata, T., 2007. El Niño Modoki and its possible teleconnection. J. Geophys. Res. 112 https://doi.org/10.1029/2006JC003798.

Beck, C., Manalt, F., Chapron, E., van Rensbergen, P., de Batist, M., 1996. Enhanced seismicity in the early post-glacial period: evidence from the post-Würm sediments of Lake Annecy, northwestern Alps. J. Geodyn. 22, 155–171.

Blaauw, M., Christen, J.A., 2011. Flexible paleoclimate age-depth models using an autoregressive gamma process. Bayesian Anal. 6, 457–474. https://doi.org/10.1214/11-BA618.

Brakenridge, G.R., 2015. Global Active Archive of Large Flood Events: Dartmouth Flood Observatory. University of Colorado. http://floodobservatory.colorado.edu/Archives/index.html.

Broccoli, A.J., Dahl, K.A., Stouffer, R.J., 2006. Response of the ITCZ to northern hemispheric cooling. Geophys. Res. Lett. 33 https://doi.org/10.1029/2005GL024546.

Cai, W., Borlace, S., Lengaigne, M., van Rensch, P., Collins, M., Vecchi, G., Timmermann, A., Santoso, A., McPhaden, M.J., Wu, L., England, M.H., Wang, G., Guilyardi, E., Jin, F.-F., 2014. Increasing frequency of extreme El Niño events due to greenhouse warming. Nat. Clim. Chang. 4, 111–116. https://doi.org/10.1038/NCLIMATE2100.

Cai, W., Wang, G., Santoso, A., McPhaden, M.J., Wu, L., Jin, F.-F., Timmermann, A., Collins, M., Vecchi, G., Lengaigne, M., England, M.H., Dommenget, D., Takahashi, K., Guilyardi, E., 2015. Increased frequency of extreme La Niña events under greenhouse warming. Nat. Clim. Chang. 5, 132–137. https://doi.org/10.1038/NCLIMATE2492.

Cane, M.A., 2005. The evolution of El Niño, past and future. Earth Planet. Sci. Lett. 230, 227–240. https://doi.org/10.1016/j.epsl.2004.12.003.

Christensen, J.H., Krishna Kumar, K., Aldrian, E., An, S.-I., Cavalcanti, I.F.A., de Castro, M., Dong, W., Goswami, P., Hall, A., Kanyanga, J.K., Kitoh, A., Kossin, J., Lau, N.-C., Renwick, J., Stephenson, D.B., Xie, S.-P., Zhou, T., 2013. Climate phenomena and their relevance for future regional climate change. In: Stocker, T.F., Qin, D., Plattner, G.-K., Tignor, M., Allen, S.K., Boschung, J., Nauels, A., Xia, Y., Bex, V., Midgley, P.M. (Eds.), The Physical Science Basis. Contribution of Working Group I to the Fifth Assessment Report of the Intergovernmental Panel on Climate Change. Cambridge University Press, Cambridge, United Kingdom and New York, NY, USA.

Clement, A.C., Seager, R., Cane, M.A., Zebiak, S.E., 1996. An ocean dynamical thermostat. J. Clim. 9, 2190–2196. https://doi.org/10.1175/1520-0442(1996)009<2190:AODT>2.0.CO;2.

Cobb, K.M., Westphal, N., Sayani, H.R., Watson, J.T., Di Lorenzo, E., Cheng, H., Edwards, R.L., Charles, C.D., 2013. Highly variable El Niño–southern oscillation throughout the Holocene. Science 339, 67–70. https://doi.org/10.1126/science.1228246.

Conroy, J.L., Overpeck, J.T., Cole, J.E., Shanahan, T.M., Steinitz-Kannan, M., 2008. Holocene changes in eastern tropical Pacific climate inferred from a Galápagos lake sediment record. Quat. Sci. Rev. 27, 1166–1180. https://doi.org/10.1016/j.quascirev.2008.02.015.

Dean, W.E., 1974. Determination of carbonate and organic matter in calcareous sediments and sedimentary rocks by loss on ignition: comparison with other methods. J. Sediment. Petrol. 44, 242–248. https://doi.org/10.1306/74D729D2-2B21-11D7-8648000102C1865D.

Hendon, H.H., 2003. Indonesian rainfall variability: impacts of ENSO and local air-sea interaction. J. Clim. 16, 1775–1790. https://doi.org/10.1175/1520-0442(2003)016<1775:IRVIOE>2.0.CO;2.

Konecky, B.L., Russell, J.M., Rodysill, J.R., Vuille, M., Bijaksana, S., Huang, Y., 2013. Intensification of southwestern Indonesian rainfall over the past millennium. Geophys. Res. Lett. 40, 386–391. https://doi.org/10.1029/2012GL054331.

Ljungqvist, F.C., 2010. A new reconstruction of temperature variability in the extra-tropical Northern Hemisphere during the last two millennia. Geogr. Ann. 92, 339–351. https://www.jstor.org/stable/40930999.

Makou, M.C., Eglinton, T.I., Oppo, D.W., Hughen, K.A., 2010. Postglacial changes in El Niño and La Niña behavior. Geology 38, 43–46. https://doi.org/10.1130/G30366.1.

Masson-Delmotte, V., Schulz, M., Abe-Ouchi, A., Beer, J., Ganopolski, A., González Rouco, J.F., Jansen, E., Lambeck, K., Luterbacher, J., Naish, T., Osborn, T., Otto-Bliesner, B., Quinn, T., Ramesh, R., Rojas, M., Shao, X., Timmermann, A., 2013. Information from paleoclimate archives. In: Stocker, T.F., Qin, D., Plattner, G.-K., Tignor, M., Allen, S.K., Boschung, J., Nauels, A., Xia, Y., Bex, V., Midgley, P.M. (Eds.), The Physical Science Basis. Contribution of Working Group I to the Fifth Assessment Report of the Intergovernmental Panel on Climate Change. Cambridge University Press, Cambridge, United Kingdom and New York, NY, USA.

Moy, C.M., Seltzer, G.O., Rodbell, D.T., Anderson, D.M., 2002. Variability of El Niño/southern oscillation activity at millennial timescales during the Holocene epoch. Nature 420, 162–165. https://doi.org/10.1038/nature01194.

Oppo, D.W., Rosenthal, Y., Linsley, B.K., 2009. 2,000-year-long temperature and hydrology reconstructions from the Indo-Pacific warm pool. Nature 460, 1113–1116. https://doi.org/10.1038/nature08233.

Otto-Bliesner, B.L., Brady, E.C., Fasullo, J., Jahn, A., Landrum, L., Stevenson, S., Rosenbloom, N., Mai, A., Strand, G., 2016. Climate variability and change since 850 CE: an Ensemble approach with the community Earth system model. Bull. Am. Meteorol. Soc. 97, 735–754.

Poesponegoro, M.D., Notosusanto, N., 1984. Sejarah Nasional Indonesia (Indonesian National history) book IV. In: PN Balai Pustaka, Jakarta, Indonesia.

Richey, J.N., Sachs, J.P., 2016. Precipitation changes in the western tropical Pacific over the past millennium. Geology 44, 671–674. https://doi.org/10.1130/G37822.1.

Rodysill, J.R., Russell, J.M., Bijaksana, S., Brown, E.T., Safiuddin, L.O., Eggermont, H., 2012. A paleolimnological record of rainfall and drought from East Java, Indonesia during the last 1,400 years. J. Paleolimnol. 47, 125–139. https://doi.org/10.1007/s10933-011-9564-3.

Rodysill, J.R., Russell, J.M., Crausbay, S.D., Bijaksana, S., Vuille, M., Edwards, R.L., Cheng, H., 2013. A severe drought during the last millennium in East Java, Indonesia. Quat. Sci. Rev. 80, 102–111. https://doi.org/10.1016/j.quascirev.2013.09.005.

Ropelewski, C.F., Jones, P.D., 1987. An extension of the Tahiti-Darwin southern oscillation index. Mon. Weather Rev. 115, 2161–2165.

Rustic, G.T., Koutavas, A., Marchitto, T.M., Linsley, B.K., 2015. Dynamical excitation of the tropical Pacific Ocean and ENSO variability by little ice age cooling. Science 350, 1537–1541. https://doi.org/10.1126/science.aac9937.

Sachs, J.P., Sachse, D., Smittenberg, R.H., Zhang, Z., Battisti, D.S., Golubic, S., 2009. Southward movement of the Pacific intertropical convergence zone AD 1400-1850. Nat. Geosci. 2, 519–525. https://doi.org/10.1038/NGEO554.

Sandgren, P., Snowball, I., 2001. Application of mineral magnetic techniques to paleolimnology. In: Last, W.M., Smol, J.P. (Eds.), Tracking Environmental Change Using Lake Sediments, vol. 2. Kluwer Academic Publishers, Dordrecht, The Netherlands ch. 8.

Schneider, T., Hampel, H., Mosquera, P.V., Tylmann, W., Grosjean, M., 2018. Paleo-ENSO revisited: Ecuadorian Lake Pallcacocha does not reveal a conclusive El Niño signal. Glob. Planet. Chang. 168, 54–66. https://doi.org/10.1016/j.gloplacha.2018.06.004.

Stevenson, S., Capotondi, A., Fasullo, J., Otto-Bliesner, B., 2017. Forced changes to twentieth century ENSO diversity in a last Millennium context. Clim. Dyn. 52, 7359–7374. https://doi.org/10.1007/s00382-017-3573-5.

Thompson, D.M., Conroy, J.L., Collins, A., Hlohowskyj, S.R., Overpeck, J.T., Riedinger-Whitmore, M., Cole, J.E., Bush, M.B., Whitney, H., Corley, T.L., Kannan, M.S., 2017. Tropical pacific climate variability over the last 6000 years as recorded in Bainbridge Crater lake. Galápagos: Paleoceanography 32, 903–922. https://doi.org/10.1002/2017PA003089.

Tierney, J.E., Oppo, D.W., Rosenthal, Y., Russell, J.M., Linsley, B.K., 2010. Coordinated hydrological regimes in the Indo-Pacific region during the past two millennia. Paleoceanography 25. https://doi.org/10.1029/2009PA001871.

Vecchi, G.A., Wittenberg, A.T., 2010. El Niño and our future climate: where do we stand? Wiley Interdiscip. Rev. Clim. Chang. 1, 260–270. https://doi.org/10.1002/wcc.33.

Vose, R.S., Schmoyer, R.L., Steurer, P.M., Peterson, T.C., Heim, R., Karl, T.R., Eischeid, J.K., 1992. Long-term Monthly Temperature, Precipitation, Sea Level Pressure, and Station Pressure Data: the Global Historical Climatology Network, ORNL/CDIAC-53, NDP-041, Carbon Dioxide Information Analysis Center. Oak Ridge National Laboratory, Oak Ridge, Tennessee.

Wang, Y., Cheng, H., Edwards, R.L., He, Y., Kong, X., An, Z., Wu, J., Kelly, M.J., Dykoski, C.A., Li, X., 2005. The Holocene Asian monsoon: links to solar changes and north Atlantic climate. Science 308, 854–857. https://doi.org/10.1126/science.1106296.

Yan, H., Wei, W., Soon, W., An, Z., Zhou, W., Liu, Z., Wang, Y., Carter, R.M., 2015. Dynamics of the intertropical convergence zone over the western pacific during the little ice age. Nat. Geosci. 8, 315–320. https://doi.org/10.1038/NGEO2375.

Zhang, P., Cheng, H., Edwards, R.L., Chen, F., Wang, Y., Yang, X., Liu, J., Tan, M., Wang, X., Liu, J., An, C., Dai, Z., Zhou, J., Zhang, D., Jia, J., Jin, L., Johnson, K.R., 2008. A test of climate, sun, and culture relationships from an 1810-yr Chinese cave record. Science 322, 940–942. https://doi.org/10.1126/science.1163965.